

## Supporting Information

# Modulation of junction modes in SnSe<sub>2</sub>/MoTe<sub>2</sub> broken-gap van der Waals heterostructure

*Juchan Lee<sup>†,#</sup>, Ngoc Thanh Duong<sup>†,#</sup>, Seungho Bang<sup>†</sup>, Chulho Park<sup>†</sup>, Duc Anh Nguyen<sup>†</sup>, Hobeom Jeon<sup>†</sup>, Jiseong Jang<sup>†</sup>, Hye Min Oh<sup>†,\*</sup>, and Mun Seok Jeong<sup>†,\*</sup>*

<sup>†</sup>Department of Energy Science, Sungkyunkwan University, Suwon 16419, Republic of Korea

<sup>#</sup> These authors contributed equally to this study

<sup>\*</sup>Corresponding authors: ohmin@skku.edu, mjeong@skku.edu

KEYWORDS: transition-metal dichalcogenides, tunnel diode, van der Waals heterostructure, photo-voltaic effect, infrared photo-detector, broken-gap band alignment, anisotype heterojunction

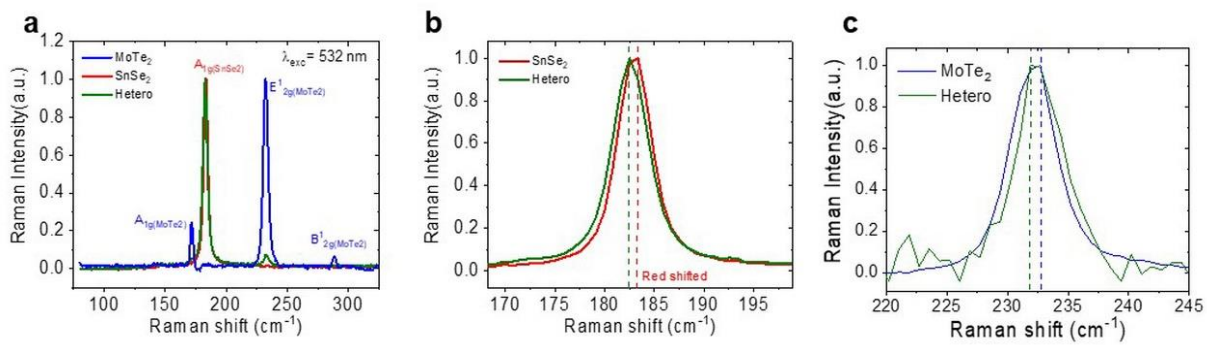


**Figure S1.** (a) Raman scattering spectra of MoTe<sub>2</sub>, SnSe<sub>2</sub>, and heterojunction measured with a 532-nm laser excitation. (b)  $A_{1g}$  peaks of SnSe<sub>2</sub> measured in the pristine SnSe<sub>2</sub> and heterojunction regions. (c)  $E_{2g}^1$  peaks of MoTe<sub>2</sub> measured in the pristine MoTe<sub>2</sub> and heterojunction regions.

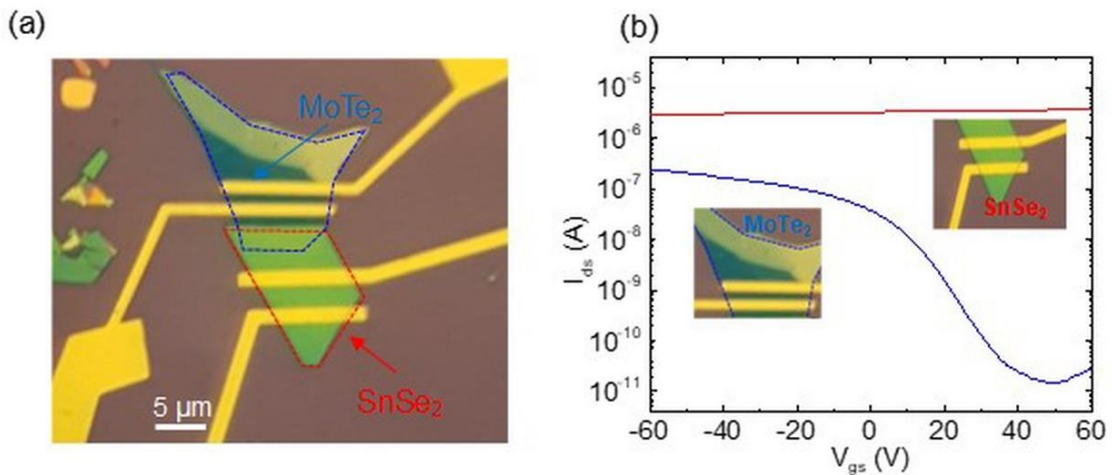


**Figure S2.** (a) Optical image of the MoTe<sub>2</sub>/SnSe<sub>2</sub> heterostructure. (b)  $I_{ds}$ – $V_{gs}$  characteristics of the single MoTe<sub>2</sub> and SnSe<sub>2</sub> FETs.

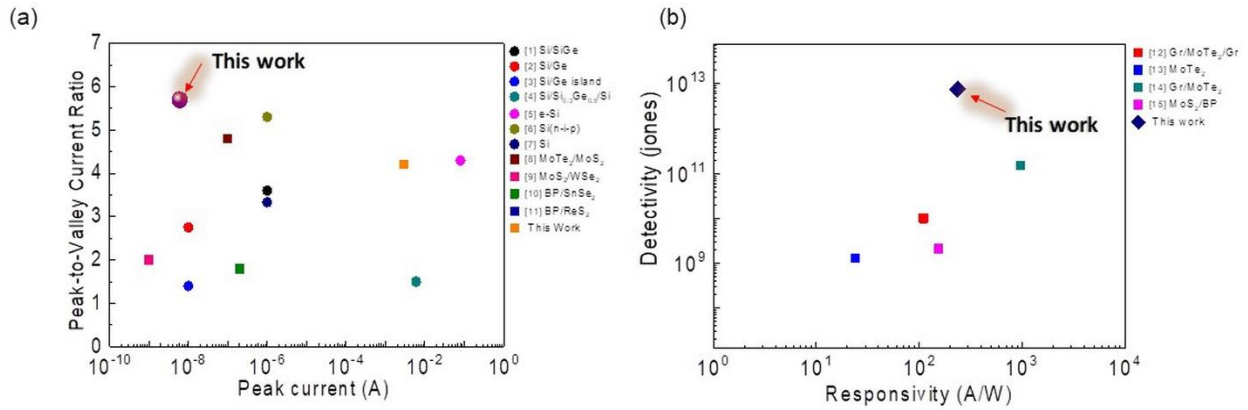


**Figure S3.** (a) PVCR–peak current and (b) detectivity–responsivity results of this and recent studies.

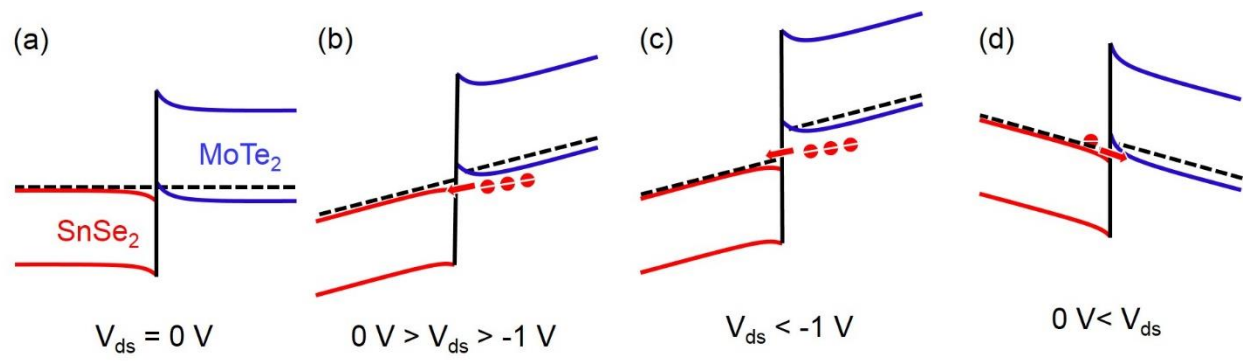


**Figure S4.** Band alignments of the MoTe<sub>2</sub>/SnSe<sub>2</sub> heterojunction in the accumulation mode at various  $V_{ds}$  values: (a)  $V_{ds} = 0$  V (equilibrium), (b)  $0 \text{ V} > V_{ds} > -1 \text{ V}$  (small reverse bias), (c)  $V_{ds} < -1 \text{ V}$ , (d)  $0 \text{ V} < V_{ds}$  (forward bias).

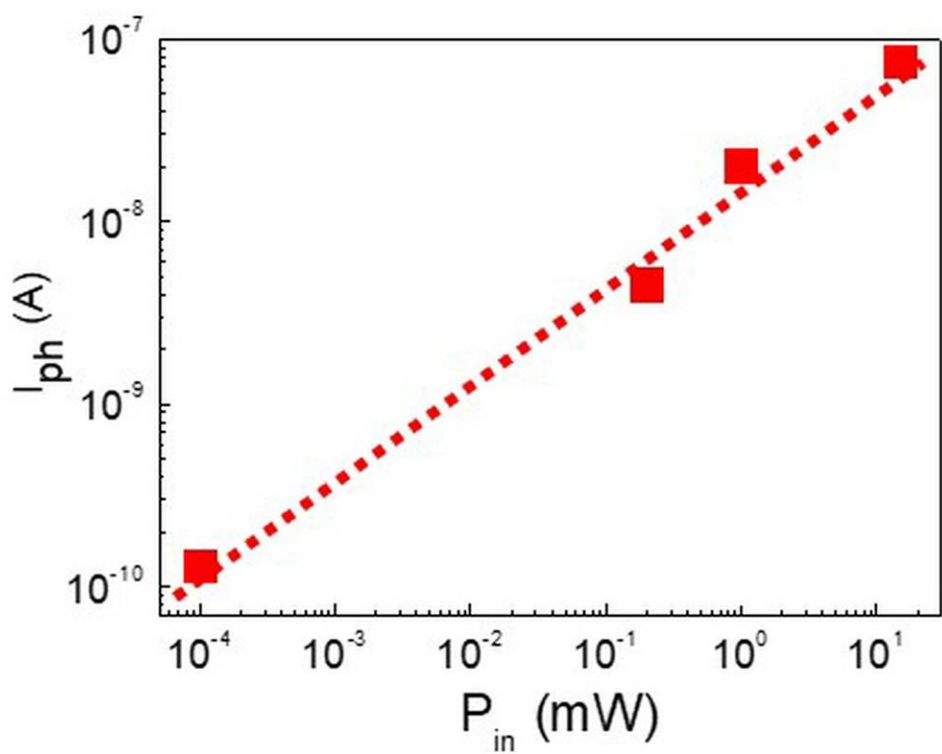


**Figure S5.** Linear variation in photo-current  $I_{\text{ph}}$  with the laser power  $P_{\text{in}}$ .

## References:

1. Jin, N.; Chung, S.-Y.; Rice, A. T.; Berger, P. R.; Thompson, P. E.; Rivas, C.; Lake, R.; Sudirgo, S.; Kempisty, J. J.; Curanovic, B. *IEEE Transactions on Electron Devices* **2003**, 50, (9), 1876-1884.
2. Fung, W. Y.; Chen, L.; Lu, W. *Applied Physics Letters* **2011**, 99, (9), 092108.
3. Schmidt, O.; Denker, U.; Eberl, K.; Kienzle, O.; Ernst, F.; Haug, R. J. *Applied Physics Letters* **2000**, 77, (26), 4341-4343.
4. Rommel, S. L.; Dillon, T. E.; Dashiell, M.; Feng, H.; Kolodzey, J.; Berger, P. R.; Thompson, P. E.; Hobart, K. D.; Lake, R.; Seabaugh, A. C. *Applied Physics Letters* **1998**, 73, (15), 2191-2193.
5. Fave, A.; Lelièvre, J.-F.; Gallet, T.; Su, Q.; Lemiti, M. *Energy Procedia* **2017**, 124, 577-583.
6. Oehme, M. *Thin Solid Films* **2012**, 520, (8), 3341-3344.
7. Oehme, M.; Kirfel, O.; Werner, J.; Kaschel, M.; Kasper, E.; Schulze, J. *Thin Solid Films* **2010**, 518, (6), S65-S67.
8. Duong, N. T.; Bang, S.; Lee, S. M.; Dang, D. X.; Kuem, D. H.; Lee, J.; Jeong, M. S.; Lim, S. C. *Nanoscale* **2018**, 10, (26), 12322-12329.
9. Roy, T.; Tosun, M.; Cao, X.; Fang, H.; Lien, D.-H.; Zhao, P.; Chen, Y.-Z.; Chueh, Y.-L.; Guo, J.; Javey, A. *ACS nano* **2015**, 9, (2), 2071-2079.
10. Yan, R.; Fathipour, S.; Han, Y.; Song, B.; Xiao, S.; Li, M.; Ma, N.; Protasenko, V.; Muller, D. A.; Jena, D. *Nano letters* **2015**, 15, (9), 5791-5798.
11. Shim, J.; Oh, S.; Kang, D.-H.; Jo, S.-H.; Ali, M. H.; Choi, W.-Y.; Heo, K.; Jeon, J.; Lee, S.; Kim, M. *Nature communications* **2016**, 7, 13413.
12. Zhang, K.; Fang, X.; Wang, Y.; Wan, Y.; Song, Q.; Zhai, W.; Li, Y.; Ran, G.; Ye, Y.; Dai, L. *ACS applied materials & interfaces* **2017**, 9, (6), 5392-5398.
13. Huang, H.; Wang, J.; Hu, W.; Liao, L.; Wang, P.; Wang, X.; Gong, F.; Chen, Y.; Wu, G.; Luo, W. *Nanotechnology* **2016**, 27, (44), 445201.
14. Yu, W.; Li, S.; Zhang, Y.; Ma, W.; Sun, T.; Yuan, J.; Fu, K.; Bao, Q. *Small* **2017**, 13, (24), 1700268.
15. Ye, L.; Li, H.; Chen, Z.; Xu, J. *Acs Photonics* **2016**, 3, (4), 692-699.